*Life-Cycle of Structures and Infrastructure Systems – Biondini & Frangopol (Eds)*


# Structural behaviour of axially loaded corroded low-strength RC columns with different confinement ratios

H.O. Aminulai, N.S. Ferguson & M.M. Kashani
*University of Southampton, Southampton, UK*

ABSTRACT: Many ageing structures in earthquake-prone regions are vulnerable to failure by seismic actions resulting from poor detailing, environmental degradation and quality of materials used. Insufficient column confinement and corrosion of the embedded rebars have been identified as some of the problems with structures in such environments leading to severe damage during earthquakes. This paper presents summary of the result of an experimental investigation on low-strength reinforced concrete (RC) columns with different confinement levels and varying degrees of corrosion. The experiment was done on 20 short RC columns (10 squares and 10 circulars) with two confinements ratios and steel corrosion loss (0% to 30%) subjected to monotonic axial load. The result showed that the axial load carrying capacity and ductility of corroded RC columns reduced with increased in the corrosion mass loss ratios.

## 1 INTRODUCTION

Over time, the ageing in reinforced concrete (RC) structures results in the degradation of the engineering properties of structures by limiting the capacity and resistance to failure (Karapetrou et al., 2017, Yang et al., 2016). This failure is more pronounced in RC structures in aggressive and marine environments located in seismic regions subject to corrosion effects and poor quality of materials used in construction. Corrosion of reinforcement in concrete is one of the most common and dangerous environmental deteriorations affecting the structural performance of ageing structures in chloride-laden and high seismic environments (Kashani et al., 2015a, Vu et al., 2017). Furthermore, it significantly reduces the diameter (Du et al., 2005), strength (Vu and Bing, 2018) and axial load-bearing capacity of reinforcing bars in corroded RC structures (Shen et al., 2021), which further results in the reduction in the concrete core confinement leading to the degradation in ductility and the long-term performance of the RC structure (Ma et al., 2022, Fang, 2020). Chloride-induced corrosion significantly degrades RC structures, resulting in substantial economic loss worldwide (Altoubat et al., 2016). For example, the United States of America reported needing about $125 billion to repair ageing and existing bridges (American Society of Civil Engineers (ASCE), 2021). In comparison, the United Kingdom estimated the cost of corrosion damages to highway bridges in Wales and England (approximately 10% of the total bridges in the United Kingdom) at £1 billion per year (Wallbank, 1989).

Ageing RC columns/piers generally fail through the buckling of the vertical reinforcement bars together with the crushing of core confined concrete and the fracture of the longitudinal bars (Kashani et al., 2019), resulting from inadequate confining transverse reinforcements. This confinement reinforcement provides the compressed concrete with higher flexibility and stability, which helps to prevent collapse during vibrations (Mander et al., 1988). Thus, the higher the level of confining stress in the concrete, the more its ductility and strength gain (Zeng, 2017).

Several numerical and analytical models have been developed to investigate the effect of confinement on the axial load capacity and stress-strain behaviour of RC columns (Zeng, 2017, Saatcioglu and Razvi, 1992, Mander et al., 1988, Liang et al., 2015, Hoshikuma et al., 1997). However, these models are primarily on plain normal and high-strength RC columns without considering the effect of corrosion. These models have been incorporated into design guidelines for new RC bridge columns/piers. However, many inadequately confined old bridge columns with low concrete strength are still in the seismic regions. Therefore, their response to the combined effects of degradation and axial load needs to be investigated.

DOI: 10.1201/9781003323020-409

The stress-strain responses of non-corroded RC columns have been extensively investigated numerically (Andisheh et al., 2021). Still, there are very few experimental investigations of the effects of corrosion on the stress-strain behaviour of confined concrete columns. This research presents the results of an experiment on ageing low-strength circular and square RC columns subject to reinforcement corrosion, confinement ratios and axial load. Twenty low-strength RC columns were designed and grouped into five targeted corrosion losses (i.e., 0%, 5%, 10%, 20% and 30%) with two confinement ratios (L/D = 5 and L/D = 13) under monotonic axial load. The different degrees of reinforcement corrosion was obtained by accelerated corrosion technique using the electrochemical process. In addition, the effect of reinforcement corrosion and confinement ratios on the load-deformation responses of the RC columns was analysed.

## 2 METHODOLOGY

### 2.1 *Specimen details and material properties*

A total of twenty RC columns (ten squares and ten circulars) were designed, as shown in Figure 1, with two confinement levels and five targeted corrosion losses. The square columns are 125 × 125 × 600mm, incorporating 4 No. 10mm diameter longitudinal bars, while the circular samples (125mm diameter × 600mm long) have 5 No. 10mm longitudinal bars. The columns were designed with two different confinement ratios in the middle 400mm zone, while the 100mm ends have transverse bars spaced at 25mm (Figures 1a and 1b). Furthermore, the 100mm ends are wrapped with epoxy-coated GFRP to prevent localised damage at the top and bottom ends of the columns and ensure that the failure occurs at the RC columns' middle zone. All the rebars in the columns were connected with tie wires to ensure that the transverse and longitudinal bars corrode simultaneously during the corrosion process.

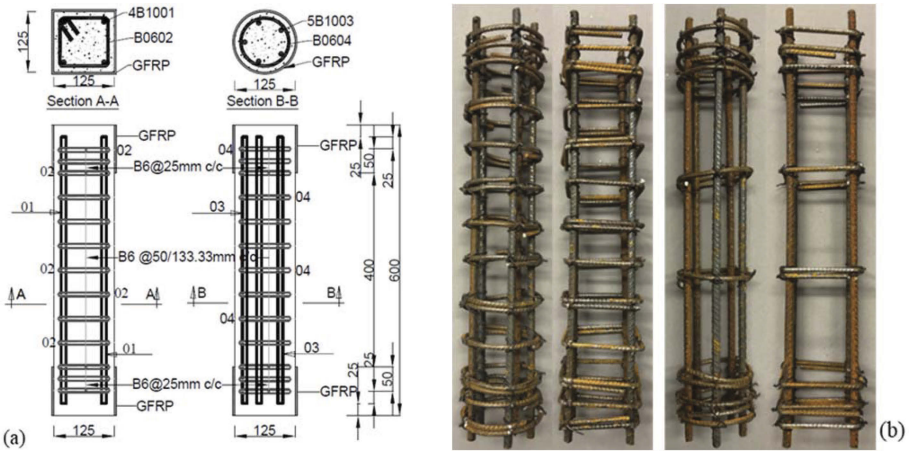


Figure 1. Specimen details; (a) schematic drawing and (b) Reinforcement layouts (cages) of the high and low confinement (circular and square columns).

The concrete was designed as low-strength concrete representing a non-code conforming column with an expected mean compressive strength of 20MPa and a nominal cover of 10mm. Compressive strength tests was done on concrete samples collected during the casting of the columns at the Testing and Structures Research Laboratory (TSRL), University of Southampton, using the servo-hydraulic 630kN Instron Schenk machine. The columns were tested using the displacement control at a constant loading rate of 1mm/min until failure. The samples used for this test were not the conventional cube/cylinder samples but with the same configurations as the reinforced ones. The compressive strength of the concrete is estimated to be 12.1MPa.

### 2.2 *Accelerated corrosion procedure*

The natural corrosion process usually takes a more extended period which could be several years or decades (Kashani et al., 2019). As such, the electrochemical process known as the accelerated corrosion method is often adopted in the laboratory to simulate the corrosion process. The RC samples' corrosion was done by passing a constant current of 2A through the reinforcing bars connected to the anode of the DC power supplies while also connecting the stainless steel plate to the cathode. Then, the connected specimen is placed in a salt bath with 10% sodium chloride (NaCl) by water weight to simulate the corrosive environment (Figure 2 (a and b)).

This process is used to get an estimated corrosion mass loss by calculating the duration expected to achieve the desired mass loss using Faraday's 2nd law of electrolysis (Equation 1) (Kashani et al., 2013b). Conversely, the actual mass loss is estimated at the end of testing by weighing the rebars after removing and cleaning the rust and concrete from the surface (Equation 2). Equation 2 gives an average corrosion loss (mass loss) along the length of the rebar.

$$\Delta m = \frac{MIT}{ZF} \tag{1}$$

$$\gamma = \frac{m_0 - m}{m} \times 100 \tag{2}$$

where $\Delta m$ = mass loss (g), M = molar mass of iron (56g/mol), Z = ionic charge for iron, F = Faraday's constant (96500 C/mol), I = applied current (A), T = time to achieve corrosion (s), $m_0$, = mass per unit length of original rebar, and $m$ = mass per unit length of the corroded rebar.

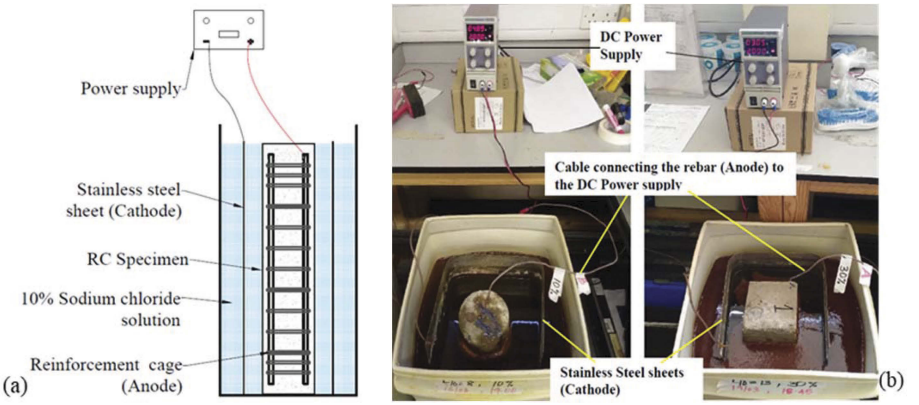


Figure 2. Accelerated corrosion procedure; (a) Schematic setup drawing, (b) laboratory setup.

## 3 EXPERIMENTAL SETUP

This experiment studies the response of low-strength RC columns to axial compressive loading using the servo-hydraulic 630kN capacity Instron Schenck machine having a 250mm travel at the Testing and Structures Research Laboratory (TSRL) of the University of Southampton. The test is conducted at a constant loading rate of 1mm/min using the displacement control settings in the Instron software. The laboratory setup of the experiment is shown in Figure 3(a). The displacement at the middle section of the column is measured with two Linear Variable Differential Transformers (LVDT) fixed to the edge of the GFRP strengthened end Figure 3(b-c).

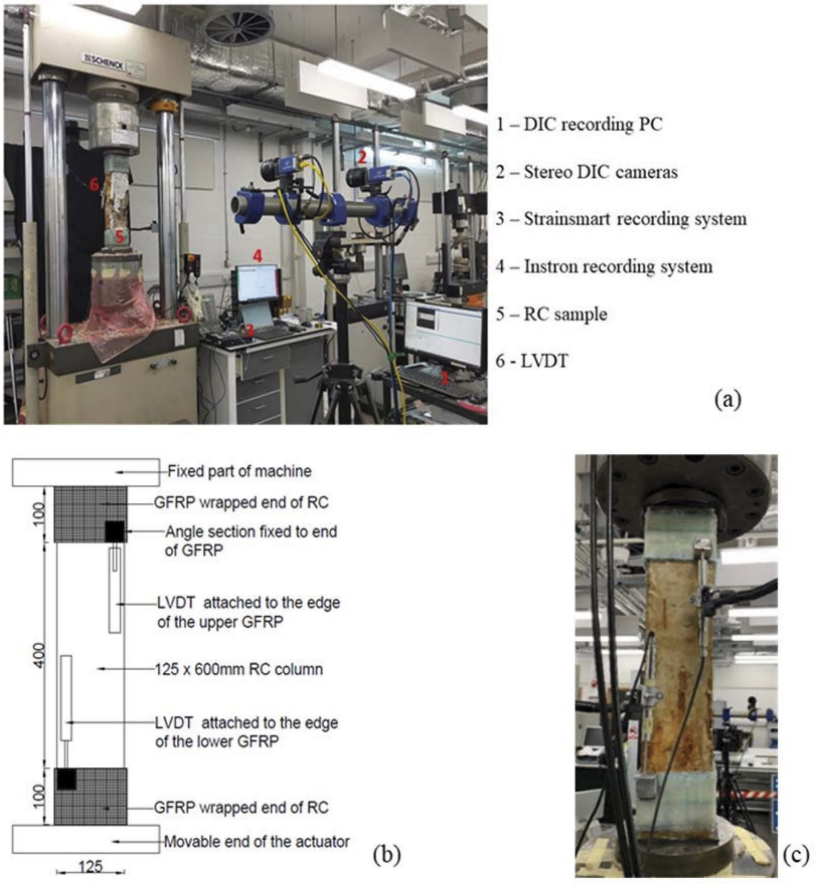


Figure 3. Experimental test setup (a) laboratory setup; (b) schematic of the LVDT connection; (c) Image of the LVDT connections to the RC samples.

## 4 EXPERIMENTAL RESULTS

### 4.1 *Calculation of corrosion and mass loss ratio*

The mass loss results are illustrated in Table 1 for the circular and square columns. The results indicate that the transverse stirrups had more severe corrosion than the longitudinal bar under the same constant current and duration (Li et al., 2022). This results from the closeness of the transverse bars to the surface of the concrete, leading to a possibly higher concentration of chloride ions and an early start of corrosion (Gu et al., 2020). Furthermore, the diameter of the longitudinal rebar (10mm) was greater than that of the stirrups (6mm). In this regard, the mass loss ratio of transverse stirrups with smaller diameters was higher than that of the longitudinal rebar, according to Faraday's second law of electrolysis (Kashani et al., 2013b).

### 4.2 *Axial stress-strain response of RC columns*

The stress-strain responses of the circular and square columns to the applied axial compressive load are presented in Figures 4 (a-b) and 4 (c-d). The stress-strain response plotted was from the LVDTs data, which captures the deformation of the sample at the 400mm middle section. The compressive response of the columns is similar at the elastic range until yield and afterwards reduces beyond the peak load due to corrosion and confinements of the rebars (Dong et al., 2018).

Table 1. Corrosion properties of the RC columns.

| Circular columns | | | | Square columns | | | |
|---|---|---|---|---|---|---|---|
| Specimen label | Estimated mass loss (Eq. 1) (%) | Measured mass loss of longitudinal bars (Eq. 2) (%) | Measured mass loss of transverse bars (Eq. 2) (%) | Specimen label | Estimated mass loss (Eq. 1) (%) | Measured mass loss of longitudinal bars (Eq. 2) (%) | Measured mass loss of transverse bars (Eq. 2) (%) |
| C5B0 | 0 | 0 | 0 | S5B0 | 0 | 0 | 0 |
| C5B5 | 5 | 4.1 | 8.8 | S5B5 | 5 | 3.4 | 10.9 |
| C5B10 | 10 | 7.3 | 21.2 | S5B10 | 10 | 6.8 | 17.1 |
| C5B20 | 20 | 10.8 | 29.4 | S5B20 | 20 | 13.8 | 37.0 |
| C5B30 | 30 | 20.6 | 39.8 | S5B30 | 30 | 18.4 | 46.3 |
| C13B0 | 0 | 0 | 0 | S13B0 | 0 | 0 | 0 |
| C13B5 | 5 | 6.0 | 12.7 | S13B5 | 5 | 6.2 | 11.8 |
| C13B10 | 10 | 12.5 | 30.1 | S13B10 | 10 | 8.8 | 17.4 |
| C13B20 | 20 | 16.1 | 37.2 | S13B20 | 20 | 10.7 | 25.3 |
| C13B30 | 30 | 27.6 | 45.9 | S13B30 | 30 | 20.2 | 30.3 |

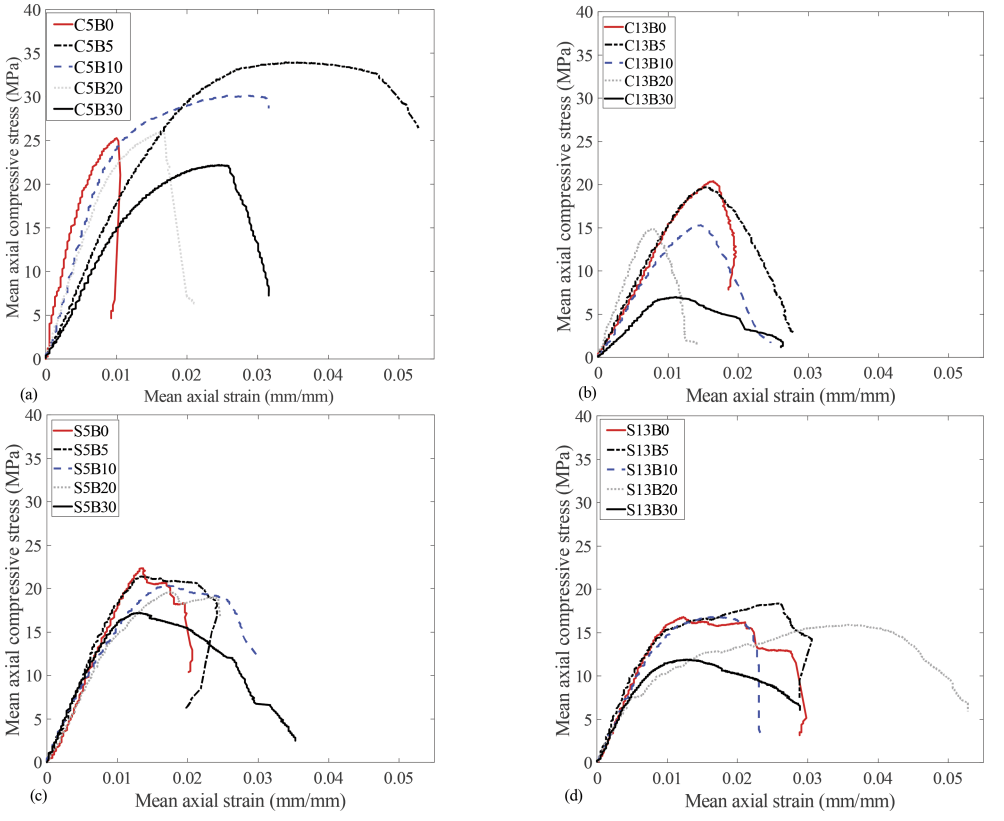


Figure 4. Axial compressive stress-strain responses of RCcolumns (a) circular L/D = 5, (b) circular L/D = 13, (c) square L/D = 5, and (d) square L/D = 13.

The axial load-carrying capacities of the columns generally decrease with an increase in the corrosion level within each confinement configuration of columns, except in some cases where the control sample (0% corrosion) recorded low capacity due to the premature failure of the strengthening GFRP at the top/bottom of the column. The failure of the GFRP at the

top/bottom of the column leads to stress concentration and premature failure of the columns. It is observed that the circular columns generally have better axial load-carrying capacities and axial strain than the square columns (Liang et al., 2015, Dizaj and Kashani, 2020). This results from the effectiveness of the transverse ties in the circular column, which has more significant confinement effectiveness coefficients than the square columns (Liang et al., 2015)

### 4.3 *Impact of corrosion on the strength of confined RC column*

The strength loss resulting from the corrosion and confinement ratios of the RC columns is determined by normalising the ultimate strength of the corroded columns to the ultimate strength of the uncorroded. The normalised strength loss of the differently confined RC columns is plotted relative to the percentage of corrosion mass loss. Linear trend lines are fitted to the test data to estimate the strength reduction due to corrosion and confinement ratios. The R-square values obtained from the trendlines are 0.95 and 0.90 for the circular columns with high and low confinement ratios, respectively, while the variation for the square columns is 0.99 and 0.96 for similarly confined columns (Figure 5). The ultimate strength of the confined corroded RC columns is reduced with an increase in the confinement degree and corrosion mass loss. For example, the high-confined circular columns (Figure 5(a)) have a strength reduction range of 4.7%, 14%, 26% and 36.7% for the 4.1%, 7.3%, 10.8% and 20.6% corrosion mass loss, respectively. Also, the high-confined square columns (Figure 5(b)) have a strength reduction range of 5.1%, 10.6%, 19.6% and 29.6% for the 3.4%, 6.8%, 13.8% and 18.4% corrosion mass loss, respectively. A similar trend is observed in the low-confined columns, with the strength reduction increasing with an increase in the corrosion mass losses in the circular and square columns.

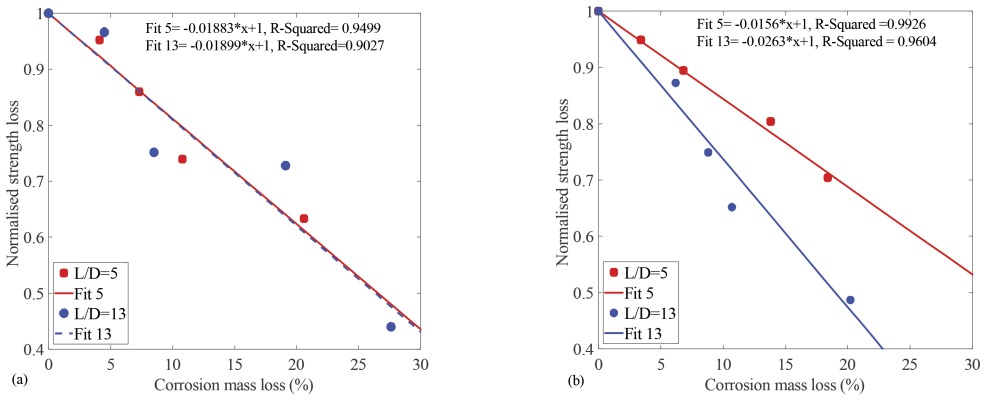


Figure 5. Strength variation of the confined RC columns with corrosion (a) circular and (b) square.

### 4.4 *Impact of corrosion on inelastic buckling behaviour of vertical reinforcement*

Corrosion generally reduces the cross-sectional areas of bars available to sustain the applied load (Kashani, 2017). This reduction becomes more severe in bars with pitting corrosion, resulting in localised reduction in the cross-sectional areas of the bars, causing rebar fracture and localised buckling. Longitudinal bars in columns with L/D = 5 confinement had less buckling failure, especially at lower corrosion than bars from the L/D = 13 configurations. The buckling from the columns with L/D = 5 rebars at higher corrosion levels results from the unsymmetrical cross-sections arising from the pitting corrosion causing imperfections in the bar and leading to additional bending moment and local stresses at the pitted sections (Kashani et al., 2013b, Kashani et al., 2013a). Meanwhile, the buckling from the columns with L/D = 13 results from the combination of pitting corrosion and inadequate confinement provisions leading to premature yielding and squashing of the weakest section even at lower corrosion degrees (Kashani et al., 2015b).

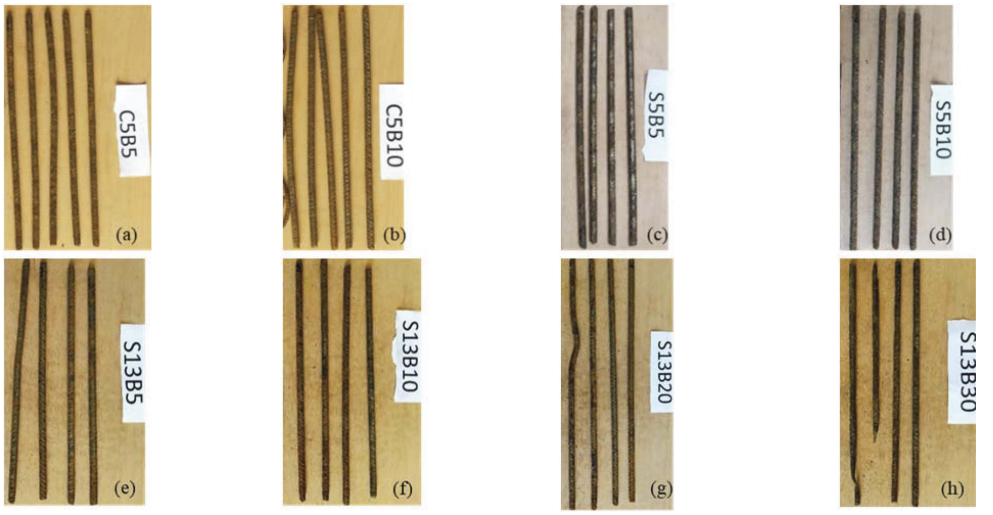


Figure 6. Observed buckling failure of the longitudinal reinforcement after testing; L/D = 5 (a-d) and L/D = 13 (e-h).

## 5 CONCLUSIONS

The effects of corrosion on the axial load capacity of differently confined RC columns have been studied experimentally. The primary conclusions drawn from the analysis of the experimental data are as follows.

Corrosion of reinforcements severely reduces the load-carrying capacity and stiffness of RC columns. Therefore, local buckling is more severe for specimens with high corrosion rates and buckling always occur in the sections with more rust products. This is evidence that the local buckling of the rebar is strongly related to its corrosion condition. Furthermore, the inelastic buckling mechanism of bars is affected by non-uniform pitting corrosion. The observed buckling modes showed that the buckling mechanism of corroded bars is a function of the mass loss due to corrosion and the distribution of pits along the bar length. Hence, the bars with more corrosion mass loss experienced more buckling and fracture than columns at low corrosion losses.

Confinement also significantly impacts corroded rebars' stress-strain response and buckling, as the high-confined columns have higher load-carrying capacities than the low-confined ones. Also, highly confined columns at low corrosion have less buckling than columns with the same confinement at high corrosion. Meanwhile, low-confined columns fail due to inadequate confinement and corrosion, even at low corrosion levels.

## REFERENCES

Altoubat, S., Maalej, M. & Shaikh, F. U. A. 2016. Laboratory Simulation of Corrosion Damage in Reinforced Concrete. *International Journal of Concrete Structures and Materials*, 10, 383–391.

American Society Of Civil Engineers (ASCE) 2021. 2021 Report Card for America's Infrastructure.

Andisheh, K., Scott, A. & Palermo, A. 2021. Effects of Corrosion on Stress-Strain Behavior of Confined Concrete. *Journal of Structural Engineering*, 147, 04021087.

Dizaj, E. A. & Kashani, M. M. 2020. Numerical investigation of the influence of cross-sectional shape and corrosion damage on failure mechanisms of RC bridge piers under earthquake loading. *Bulletin of Earthquake Engineering*, 18, 4939–4961.

Dong, H.-L., Wang, D., Wang, Z. & Sun, Y. 2018. Axial compressive behavior of square concrete columns reinforced with innovative closed-type winding GFRP stirrups. *Composite Structures*, 192, 115–125.

Du, Y. G., Clark, L. A. & Chan, A. H. C. 2005. Residual capacity of corroded reinforcing bars. *Magazine of Concrete Research*, 57, 135–147.
Fang, S. 2020. Axial Compressive Performance of Corroded Concrete Columns Strengthened by Alkali-Activated Slag Ferrocement Jackets. *Frontiers in Materials*, 7, 1–12.
Gu, X.-L., Dong, Z., Yuan, Q. & Zhang, W.-P. 2020. Corrosion of Stirrups under Different Relative Humidity Conditions in Concrete Exposed to Chloride Environment. *Journal of Materials in Civil Engineering*, 32, 04019329.
Hoshikuma, J., Kawashima, K., Nagaya, K. & Taylor, A. W. 1997. Stress-Strain Model for Confined Reinforced Concrete in Bridge Piers. *Journal of Structural Engineering*, 123, 624–633.
Karapetrou, S. T., Fotopoulou, S. D. & Pitilakisa, K. D. 2017. Seismic Vulnerability of RC Buildings under the Effect of Aging. *Procedia Environmental Sciences*, 38, 461–468.
Kashani, M. M. 2017. Size Effect on Inelastic Buckling Behavior of Accelerated Pitted Corroded Bars in Porous Media. *Journal of Materials in Civil Engineering*, 29, 04017022.
Kashani, M. M., Alagheband, P., Khan, R. & Davis, S. 2015a. Impact of corrosion on low-cycle fatigue degradation of reinforcing bars with the effect of inelastic buckling. *International Journal of Fatigue*, 77, 174–185.
Kashani, M. M., Crewe, A. J. & Alexander, N. A. 2013a. Nonlinear cyclic response of corrosion-damaged reinforcing bars with the effect of buckling. *Construction and Building Materials*, 41, 388–400.
Kashani, M. M., Crewe, A. J. & Alexander, N. A. 2013b. Nonlinear stress–strain behaviour of corrosion-damaged reinforcing bars including inelastic buckling. *Engineering Structures*, 48, 417–429.
Kashani, M. M., Lowes, L. N., Crewe, A. J. & Alexander, N. A. 2015b. Phenomenological hysteretic model for corroded reinforcing bars including inelastic buckling and low-cycle fatigue degradation. *Computers & Structures*, 156, 58–71.
Kashani, M. M., Maddocks, J. & Dizaj, E. A. 2019. Residual Capacity of Corroded Reinforced Concrete Bridge Components: State-of-the-Art Review. *Journal of Bridge Engineering*, 24, 1–16.
Li, Q., Dong, Z., He, Q., Fu, C. & Jin, X. 2022. Effects of Reinforcement Corrosion and Sustained Load on Mechanical Behavior of Reinforced Concrete Columns. *Materials (Basel)*, 15.
Liang, X., Beck, R. & Sritharan, S. 2015. Understanding the Confined Concrete Behavior on the Response of Hollow Bridge Columns. Department of Civil Construction and Environmental Engineering. Iowa State University.
Ma, J., Yu, L., Li, B. & Yu, B. 2022. Stress–strain model for confined concrete in rectangular columns with corroded transverse reinforcement. *Engineering Structures*, 267, 1–14.
Mander, J. B., Priestley, M. J. N. & Park, R. 1988. Theoretical stress-strain model for confined concrete. *Journal of Structural Engineering*, 114, 1804–1826.
Saatcioglu, M. & Razvi, S. R. 1992. Strength and Ductility of Confined Concrete. *Journal of Structural Engineering*, 118, 1590–1607.
Shen, D., Li, M., Liu, C., Kang, J., Li, C. & Yang, J. 2021. Seismic performance of corroded reinforced concrete beam-column joints repaired with BFRP sheets. *Construction and Building Materials*, 307, 124731.
Vu, N. S. & Bing, L. 2018. Seismic Performance Assessment of Corroded Reinforced Concrete Short Columns. *Journal of Structural Engineering*, 144, 1–12.
Vu, N. S., Yu, B. & Li, B. 2017. Stress-strain model for confined concrete with corroded transverse reinforcement. *Engineering Structures*, 151, 472–487.
Wallbank, E. J. The Performance of Concrete in Bridges: a Survey of 200 Highway Bridges. 1989.
Yang, S.-Y., Song, X.-B., Jia, H.-X., Chen, X. & Liu, X.-L. 2016. Experimental research on hysteretic behaviors of corroded reinforced concrete columns with different maximum amounts of corrosion of rebar. *Construction and Building Materials*, 121, 319–327.
Zeng, X. 2017. Finite Element Analysis of Square RC Columns Confined by Different Configurations of Transverse Reinforcement. *The Open Civil Engineering Journal*, 11, 292–302